



|                    |   |
|--------------------|---|
| <b>Title</b>       | <b>Loss of APD1 in Yeast Confers Hydroxyurea Sensitivity Suppressed by Yap1p Transcription Factor</b> |
| <b>Author(s)</b>   | <b>Tang, HM; Pan, K; Kong, KYE; Hu, L; Chan, LC; Siu, KL; Sun, H; Wong, CM; Jin, D</b>                |
| <b>Citation</b>    | <b>Scientific Reports, 2015, v. 5, p. 7897</b>  |
| <b>Issued Date</b> | <b>2015</b>   |
| <b>URL</b>         | <b><a href="http://hdl.handle.net/10722/215093">http://hdl.handle.net/10722/215093</a></b>            |
| <b>Rights</b>      | <b>Creative Commons: Attribution 3.0 Hong Kong License</b>  |



## OPEN

Loss of *APD1* in Yeast Confers Hydroxyurea Sensitivity Suppressed by Yap1p Transcription FactorSUBJECT AREAS:  
FUNGAL BIOLOGY  
FUNGAL GENETICS  
STRESS SIGNALLINGHei-Man Vincent Tang<sup>1,2</sup>, Kewu Pan<sup>3,4</sup>, Ka-Yiu Edwin Kong<sup>1,2</sup>, Ligang Hu<sup>5</sup>, Ling-Chim Chan<sup>1,2</sup>, Kam-Leung Siu<sup>1,2</sup>, Hongzhe Sun<sup>5</sup>, Chi-Ming Wong<sup>3,4</sup> & Dong-Yan Jin<sup>1,2,6</sup>Received  
18 September 2014Accepted  
16 December 2014Published  
20 January 2015

Correspondence and requests for materials should be addressed to C.-M.W. (wispwong@hku.hk) or D.-Y.J. (dyjin@hku.hk)

<sup>1</sup>Shenzhen Institute of Research and Innovation, The University of Hong Kong, Shenzhen, China, <sup>2</sup>Department of Biochemistry, The University of Hong Kong, Pokfulam, Hong Kong, <sup>3</sup>Department of Medicine, The University of Hong Kong, Pokfulam, Hong Kong, <sup>4</sup>State Key Laboratory of Pharmaceutical Biotechnology, The University of Hong Kong, Pokfulam, Hong Kong, <sup>5</sup>Department of Chemistry, The University of Hong Kong, Pokfulam, Hong Kong, <sup>6</sup>State Key Laboratory for Liver Research, The University of Hong Kong, Pokfulam, Hong Kong.

Ferredoxins are iron-sulfur proteins that play important roles in electron transport and redox homeostasis. Yeast Apd1p is a novel member of the family of thioredoxin-like ferredoxins. In this study, we characterized the hydroxyurea (HU)-hypersensitive phenotype of *apd1Δ* cells. HU is an inhibitor of DNA synthesis, a cellular stressor and an anticancer agent. Although the loss of *APD1* did not influence cell proliferation or cell cycle progression, it resulted in HU sensitivity. This sensitivity was reverted in the presence of antioxidant *N*-acetyl-cysteine, implicating a role for intracellular redox. Mutation of the iron-binding motifs in Apd1p abrogated its ability to rescue HU sensitivity in *apd1Δ* cells. The iron-binding activity of Apd1p was verified by a color assay. By mass spectrometry two irons were found to be incorporated into one Apd1p protein molecule. Surprisingly, ribonucleotide reductase genes were not induced in *apd1Δ* cells and the HU sensitivity was unaffected when dNTP production was boosted. A suppressor screen was performed and the expression of stress-regulated transcription factor Yap1p was found to effectively rescue the HU sensitivity in *apd1Δ* cells. Taken together, our work identified Apd1p as a new ferredoxin which serves critical roles in cellular defense against HU.

Yeast *APD1* gene is generally uncharacterized for function. It was implicated in cellular resistance to sodium ions, hydrogen peroxide, elesclomol, dithiothreitol, diamide and cumol hydroperoxide in several genome-wide studies<sup>1–3</sup>. In another global protein localization study, Apd1p was found in both the cytoplasm and the nucleus<sup>4</sup>. The interaction between Tsa1p and Apd1p was initially suggested in a large-scale mass spectrometric analysis of protein complexes in yeast<sup>5</sup>. Tsa1p is a principal peroxiredoxin and a strong suppressor of genome instability<sup>6–8</sup>. Peroxiredoxins are peroxidases that function as redox-sensitive molecular switches and tumor suppressors<sup>9–11</sup>. *TSA1*-null cells have elevated levels of dNTPs and are sensitive to hydroxyurea (HU), a dNTP depleting agent<sup>8</sup>. HU inhibits the activity of ribonucleotide reductase (RNR) by quenching the tyrosyl radical at its iron-containing active site<sup>12</sup>. RNR catalyzes the synthesis of dNTPs, the building blocks of DNA<sup>13</sup>. In addition, HU also perturbs DNA repair and elevates intracellular cGMP levels<sup>12</sup>. HU can activate several arms of cellular stress response and is commonly used as an anti-cancer agent<sup>14</sup>. As an antioxidant protein, Tsa1p requires efficient electron transfer relay to support and regenerate its functional capacity. Thioredoxins and glutaredoxins are relevant reductants to regenerate peroxiredoxins<sup>9,15–17</sup>.

Apd1p belongs to a family of thioredoxin-like ferredoxins, which has more than 100 members found in organisms ranging from bacteria to metazoan<sup>18</sup>. Ferredoxins are iron-sulfur (Fe-S) proteins that play important roles in biology<sup>19</sup>. The thioredoxin fold is also commonly found in oxidoreductases and chaperones<sup>20</sup>. Although the function of most thioredoxin-like ferredoxins remains unknown, the presence of thioredoxin fold and ferredoxin domain in these proteins is suggestive of a role in redox sensing and electron transfer. Like thioredoxins, glutaredoxins and peroxiredoxins, thioredoxin-like ferredoxins may function as thiol-based molecular switches by modulating disulfide bond formation in their target proteins<sup>16,21</sup>. In prokaryotes, thioredoxin-like ferredoxin YfaE has been suggested to be involved in diferric-tyrosyl radical maintenance in *E. coli* RNR<sup>22</sup>. More recently, yeast thioredoxin-like ferredoxins Grx3/4p and Dre2p have been characterized for their roles in supporting *in vivo* diferric tyrosyl radical formation in RNR<sup>23</sup>. That is to say, at least some thioredoxin-like ferre-

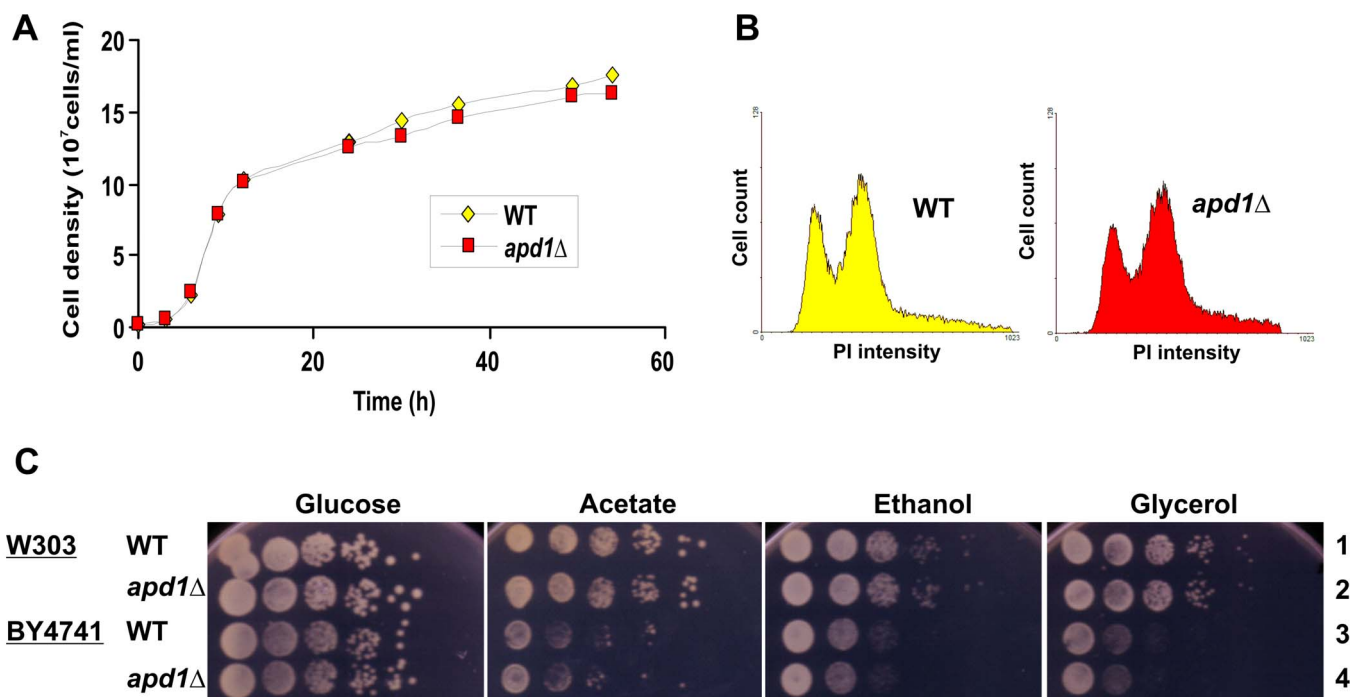


**Figure 1 | Growth and cell cycle profile of *apd1Δ* cells.** (A) Growth curve. Logarithmically growing yeast cells, BY4741 wild-type (WT) and *apd1Δ*, were inoculated in YPD medium. Cell density was determined by OD<sub>600</sub>. (B) Cell cycle profiling. Asynchronous cells of BY4741 WT and *apd1Δ* were grown to mid-log phase in YPD. Cells were fixed, treated with RNase A, and stained with propidium iodide (PI). DNA content of cells was reflected in PI intensity determined by flow cytometry. (C) Spot test in different carbon sources. Ten-fold serial dilutions of strains W303-1a WT, W303-1a *apd1Δ*, BY4741 WT and BY4741 *apd1Δ* were spotted on YP medium containing glucose, acetate, ethanol or glycerol at 2%. Plates were incubated for 3–4 days at 30°C.

doxins might play a role in redox regulation of RNR activity. It will therefore be of interest to see whether Apd1p might also serve as a redox sensor and electron carrier for RNR and/or Tsa1p.

Yap1p transcription factor and its target *ATR1* are critically involved in cellular response to oxidative stress and other cytotoxic agents<sup>24–30</sup>. Yap1p is an AP-1-like bZIP protein that controls a large and specialized stress regulon<sup>31,32</sup>. Atr1p is a multidrug resistance transporter with multiple transmembrane segments<sup>33</sup>. Both Yap1p and Atr1p are high-copy-number suppressors of cellular sensitivity to stressors such as metals, boron, reactive oxygen species, DNA damage and metabolic inhibitors<sup>24–30</sup>. Particularly, Yap1p is thought to be influential in cellular response to HU<sup>34</sup>. However, the exact roles of Yap1p and Atr1p in HU sensitivity are not known.

Characterizing Apd1p might shed light on the biological function of a family of thioredoxin-like ferredoxins. In this study we set out to perform phenotypic characterization of *apd1Δ* yeast cells and found that they are hypersensitive to HU. The iron binding capability of Apd1p was validated and shown to be important to HU resistance. The HU sensitivity in *apd1Δ* cells was suppressed by *YAP1* and *ATR1*. Our findings revealed a protective role of Apd1p in cellular defense against HU.

## Results

### APD1 is not essential for cell growth or cell cycle progression.

Genome-wide analyses revealed that loss of *APD1* in budding yeast results in cellular sensitivity to hydrogen peroxide and other stressors<sup>1–3</sup>. However, the exact biological function of *APD1* remains to be characterized. Thus, we constructed *apd1Δ* cells to study how the loss of *APD1* might affect cell growth and proliferation.

We first examined the cell growth pattern of *apd1Δ* cells. The proliferation of *apd1Δ* cells was not different from the WT BY4741 cells (Fig. 1A). Loss of *APD1* did not affect the lag phase to log phase transition or the subsequent exponential growth, suggesting that

*APD1* is non-essential to cellular growth. When we analyzed cell cycle profile by flow cytometric measurement of the DNA content of cells in asynchronous log-phase culture, both WT and *apd1Δ* cells displayed a similar DNA profile (Fig. 1B). This indicated that *APD1* is not influential on cell cycle progression. Next, we further examined the growth characteristics of WT and *apd1Δ* cells in different strain backgrounds. As shown in Fig. 1C, their growth rates and patterns were comparable in different strain backgrounds (i.e. W303-1a and BY4741) and different carbon sources (i.e. glucose, acetate, ethanol and glycerol). Thus, Apd1p has minimal influence on cell growth and cell cycle progression.

**Deletion of *APD1* sensitizes cells to hydroxyurea.** In a global protein interactome study, Apd1p was fished out by Tsa1p, a principal peroxiredoxin, suggesting a possible physical interaction and functional intersection<sup>5</sup>. From our previous work, we know that loss of *TSA1* results in elevation of dNTP levels and hypersensitivity to HU, a dNTP depleting agent<sup>8</sup>. Tsa1p is also required for the maintenance of genome stability<sup>6–8,35</sup>. Although we were unable to detect physical or genetic interaction between Apd1p and Tsa1p (data not shown), we found that loss of *APD1* also confers HU sensitivity.

We performed spot assays on agar plates containing HU and H<sub>2</sub>O<sub>2</sub> using *APD1*-proficient and -deficient cells, together with *TSA1*-null cells as positive controls. Intriguingly, deletion of *APD1* sensitized cells to HU challenge (Fig. 2A, row 2 compared to 3). This sensitivity can be fully complemented by the re-expression of *APD1* gene (Fig. 2B, row 3 compared to 1 and 2), indicating that this phenotype was due specifically to the loss of *APD1*. As a positive control, *tsa1Δ* cells were also sensitive to HU as previously described<sup>8</sup>. To our surprise but generally consistent with the lack of interaction between *APD1* and *TSA1*, *apd1Δ* cells was not sensitive to H<sub>2</sub>O<sub>2</sub> (Fig. 2A, row 2 compared to 3), while *tsa1Δ* cells became largely inviable in the

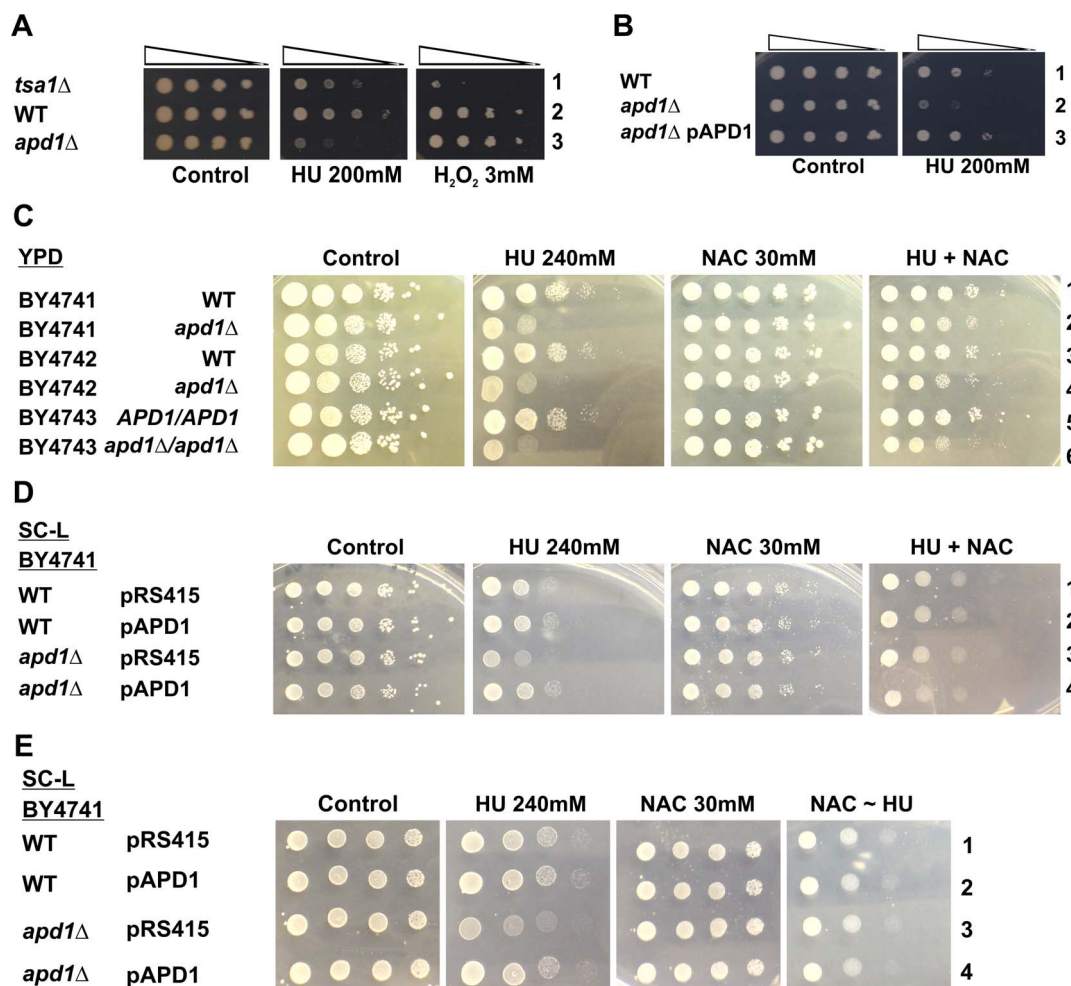


**Figure 2** | Loss of *APD1* sensitizes cells to HU. (A–B) HU sensitivity in *apd1Δ* cells. Ten-fold serial dilutions of strains BY4741 WT, BY4741 *apd1Δ* and BY4741 *tsa1Δ* (A) or BY4741 WT pRS415, BY4741 *apd1Δ* pRS415 and BY4741 *apd1Δ* pAPD1 (B) were spotted on YPD or SC-L medium containing the indicated dose of HU or H<sub>2</sub>O<sub>2</sub>. Plates were incubated for 3–4 days at 30°C. (C–D) Influence of antioxidant on HU sensitivity of haploid and diploid *apd1Δ* cells. Ten-fold serial dilutions of strains BY4741 WT, BY4741 *apd1Δ*, BY4742 WT, BY4742 *apd1Δ*, BY4743 WT and BY4743 *apd1Δ* (C) or BY4741 WT pRS415, BY4741 WT pAPD1, BY4741 *apd1Δ* pRS415 and BY4741 *apd1Δ* pAPD1 (D) were spotted on YPD or SC-L medium containing the indicated dose and combination of HU and NAC. Plates were incubated for 3–4 days at 30°C. (E) Cells were treated as in D except that cells in the (NAC ~ HU) group were treated with NAC for 12 hours and washed extensively before spotting on HU-containing plate.

presence of H<sub>2</sub>O<sub>2</sub> (Fig. 2A, row 2 compared to 1). Thus, *APD1* and *TSA1* might play distinct roles in antioxidant defense.

As a thioredoxin-like ferredoxin<sup>18</sup>, Apd1p is thought to be involved in redox regulation. Thus, we next asked whether the HU sensitivity of *apd1Δ* cells might be attributed to redox. To address this, spot assay was performed in the presence or absence of *N*-acetyl-cysteine (NAC), a potent antioxidant. The antioxidant property of NAC was first verified. When NAC was added to H<sub>2</sub>O<sub>2</sub>-treated BY4741 cells, the intracellular level of reactive oxygen species, as measured by fluorescence microscopy with the fluorescent probe 2',7'-dichlorofluorescein diacetate (DCF), was reduced (Supplementary Fig. 1, panel 5 compared to 4). In contrast, treatment with HU did not significantly affect intracellular redox (Supplementary Fig. 1, panel 6 compared to 4). Both haploid (BY4741 and BY4742) and diploid (BY4743) *apd1Δ* strains were constructed and tested (Fig. 2C, row 2 compared to 1, row 4 compared to 3, and row 6 compared to 5). Sensitivity of *apd1Δ* cells with *APD1* re-expression was also examined in the same setting (Fig. 2D, row 4 compared to 3). The HU sensitivity in *apd1Δ* cells was largely rescued by the addition of NAC (Fig. 2D, row 3 compared to 1). To rule out the possibility that NAC directly neutralizes HU in the culture medium, BY4741 cells were treated with NAC first and washed extensively before spotting

them on HU-containing agar. Similar rescuing effect was observed in these cells treated sequentially with NAC and HU (Fig. 2E, row 3 compared to 1). These results suggested that *APD1* serves as a physiological suppressor of HU sensitivity plausibly by regulating intracellular redox.

**Iron-binding motifs are critical to HU resistance.** Apd1p is a thioredoxin-like ferredoxin containing a CX<sub>3</sub>C motif and a C-terminal thioredoxin-like domain, which harbors a HX<sub>3</sub>H motif (Fig. 3A). These are iron-binding motifs resembling those found in well-characterized Fe-S clusters<sup>19</sup>.

Given that the iron-binding motifs of Apd1p might be important for function, we asked whether disrupting these motifs could affect the ability of Apd1p to rescue HU sensitivity in *APD1*-null cells. Through site-directed mutagenesis, we constructed mutants in which critical residues of the two iron-binding motifs CX<sub>3</sub>C and HX<sub>3</sub>H were altered. Plasmids expressing WT and mutant *APD1* were transformed into *apd1Δ* cells and spot assay was performed (Fig. 3B). Re-expression of *APD1* was verified at mRNA level by RT-PCR (Fig. 3C, lanes 5–7 compared to 4) and at protein level by Western blotting (Fig. 3D, lanes 4–6 compared to 3). Notably, the CX<sub>3</sub>C mutant of Apd1p could minimally rescue the HU sensitivity





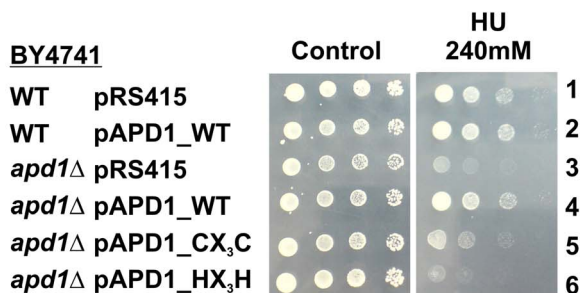
A

```

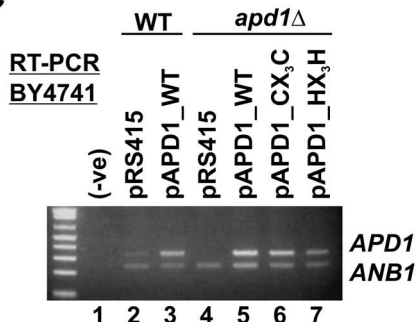
1  MAFLNIFKQK  RGDEASQLSA  KGREEISQSI  KICKSDDAAN  EHSCSGDCKT
51  EIEEGEQAFA  KLKIEHETPL  LNSSKTPKIH  FVVPTSQIDW  QHDACLEDPK
101 SVQYKISQWC  DKNSAKFSNV  GTGKTLNCAV  SSLPKDIMDI  DVMRGTKNNV
151 LILPYFIWLN  DLRSDVEAT  LDGLVPDLLD  ENISREKLE  TRPNVAVARE
201 RAFVFICSHT  TRDKRCGITA  PYLKKVFDK  LQEHGLYRDN  SDYRAEGVKI
251 AFVNHVGGHK  FAANVQIYLR  NPNTLIWLGR  VTPTIVPSIV  EHLIVPEEPT
301 LPPFEKVRCI  KKYQSW

```

B



C



D

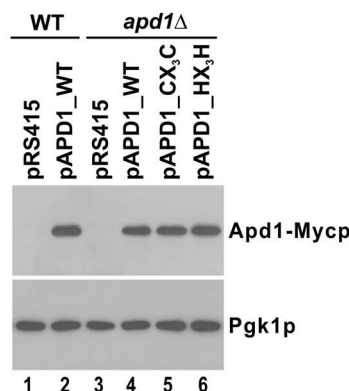


**Figure 3 | Iron-binding motifs in Apd1p are crucial to HU resistance.** (A) Primary structure of Apd1p protein. The amino acid sequence of Apd1p was retrieved from *Saccharomyces* Genome Database (SGD) with the iron-binding motifs underlined and key amino acid residues highlighted in grey. (B) Influence of iron-binding motifs of Apd1p on HU sensitivity of haploid *apd1*Δ cells. Ten-fold serial dilutions of strains WT pRS415, WT pAPD1\_WT, *apd1*Δ pRS415, *apd1*Δ pAPD1\_WT, *apd1*Δ pAPD1\_CX<sub>3</sub>C and *apd1*Δ pAPD1\_HX<sub>3</sub>H were spotted on SC-L medium containing the indicated dose of HU. Plates were incubated for 3–4 days at 30°C. Strains in the background of haploid BY4741 were used. (C) Semi-quantitative RT-PCR analysis of *APD1* transcript. Logarithmically growing cells, as indicated in A, in SC-L were harvested. Total RNA was extracted and used for cDNA synthesis. PCR was performed to assess the levels of *APD1* and *ANB1* transcripts. The housekeeping gene *ANB1* was used as an internal loading control of duplex PCR. As a negative control (-ve), no reverse transcriptase was added to the reaction in lane 1. (D) Western blot analysis of Apd1-Mycp proteins. Western blotting was performed with mouse anti-Myc (Roche) and mouse anti-Pgk1p (Invitrogen) antibodies.

(Fig. 3B, row 5 compared to 4 and 3) and the HX<sub>3</sub>H mutant was totally incapable of complementing the HU phenotype (Fig. 3B, row 6 compared to 4 and 3). Taken together, our data suggest that the two iron-binding motifs in Apd1p are indispensable for cellular defense against HU challenge.

**Apd1p is an iron-binding protein.** From genetic assays, we observed that disruption of iron-binding motifs in *APD1* perturbed its protective function against HU (Fig. 3). To formally address whether Apd1p is an iron-binding protein, we performed a series of biochemical experiments. We expressed His-Apd1p in *E. coli* and purified it to high purity as judged by SDS-PAGE (Fig. 4A). The apparent size of Apd1p was about 36 kDa which was close its predicted size (Fig. 4A). The faint band at 72 kDa might represent the dimeric form of Apd1p (Fig. 4A). To verify the presence of Fe-S cluster experimentally, we expressed and purified WT and mutant Apd1p proteins. Strikingly, Apd1p WT displayed a reddish brown color on non-denaturing PAGE gel (Fig. 4B, lane 1), indicating that

Apd1p might be an iron-binding protein. Through site-directed mutagenesis, we disrupted the iron-binding motifs in Apd1p (Fig. 3A) and generated Apd1p-CX<sub>3</sub>C and Apd1p-HX<sub>3</sub>H mutants. These two mutant proteins expressed efficiently in bacteria, but the reddish brown color was not seen in either mutant (Fig. 4B, lanes 2 and 3 compared to 1), suggesting that these motifs are critical for iron incorporation into Apd1p protein.

To corroborate that Apd1p is an iron-binding protein, the UV-visible absorption spectra of Apd1p WT and mutant proteins were obtained. Peaks at 450 nm and 570 nm were only seen in the spectrum of Apd1p WT, but not of either mutant (Fig. 4C). The absorption features were consistent with the presence of a [2Fe–2S] cluster. In further support of this, the relative amount of iron ions in Apd1p protein was determined by inductively-coupled plasma mass spectrometry (ICP-MS). The concentration of Apd1p protein was first measured by BCA micro-scale assay and iron ions were then analyzed by ICP-MS (Fig. 4D). Since 0.511 mM of iron was found in 0.268 mM of Apd1p protein solution, the Apd1p-to-Fe ratio is 1 : 1.9.

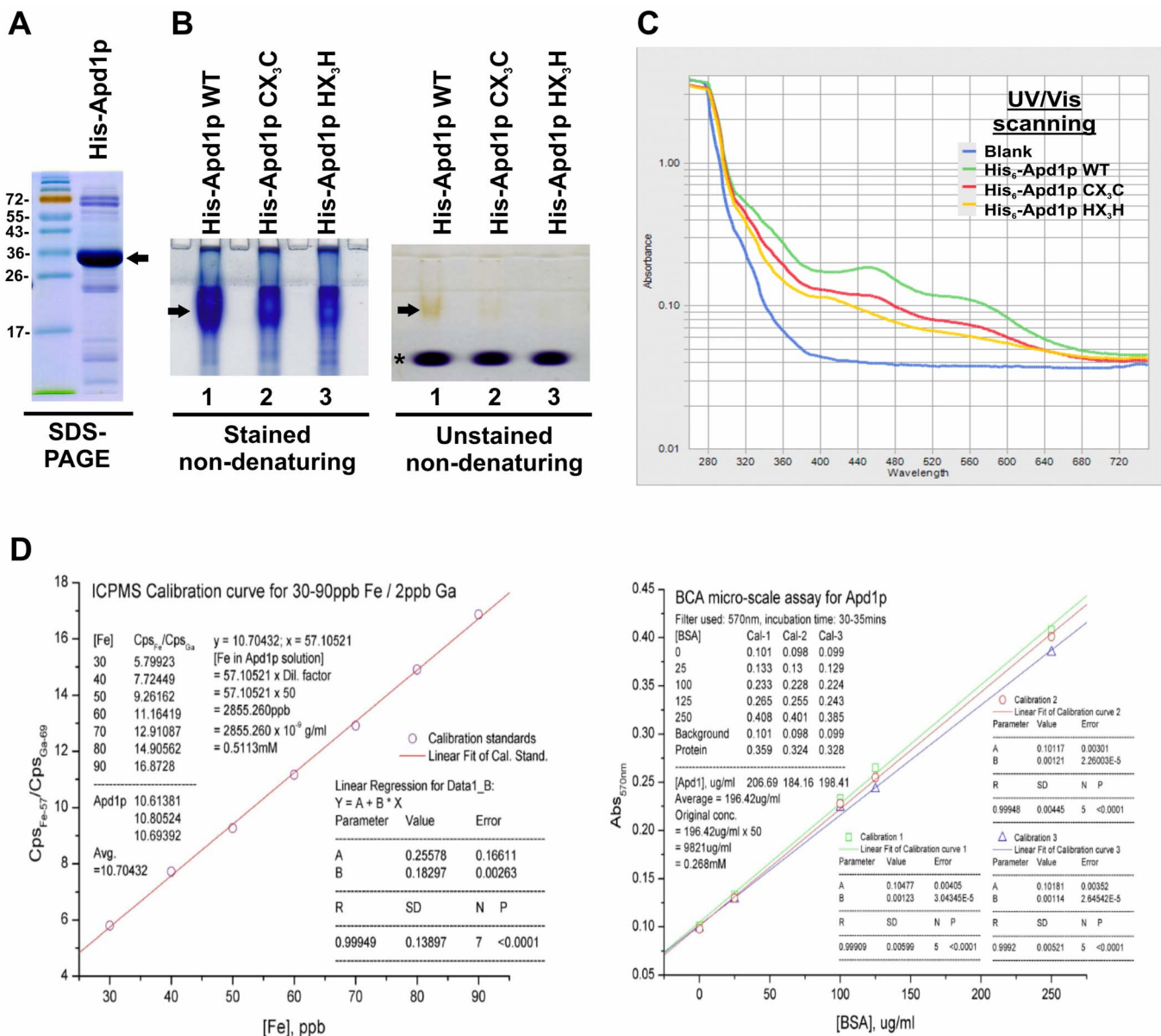


**Figure 4 | Apd1p is an iron-containing protein.** (A-B) Expression and purification of recombinant Apd1p. *E. coli*-produced recombinant His<sub>6</sub>-Apd1p was purified with Ni-NTA-Superflow resin. Proteins were eluted and subjected to 15% SDS-PAGE (for Apd1p WT) or 15% non-denaturing PAGE (for Apd1p WT, CX<sub>3</sub>C and HX<sub>3</sub>H) for size determination and color visualization, respectively. The SDS-PAGE gel was stained with Coomassie blue. The arrow points to the major Apd1p band. The asterisk denotes the dye front. The cropped non-denaturing gels are shown in the figure and the full-length gels are presented in Supplementary Figure 2. The stained and unstained gels were run under the same experimental conditions. (C) UV-visible spectra of recombinant Apd1p proteins. Purified proteins (3 mg each) were subjected to photometric scanning at the indicated wavelength range.

(D) Determination of iron concentration by ICP-MS. The concentration of Apd1p was determined by BCA micro-scale assay using BSA as a standard. To measure protein concentration of Apd1p (right panel), three calibration assays were performed with BSA to construct standard curves which represent the linear fits of experimental data. The concentration of Apd1p was then calculated to be 0.268 mM. To measure iron concentration (left panel), a set of iron standards ranging from 30 to 90 ppb was used to generate a calibration curve. Trace gallium at 2 ppb was the low calibration standard. The iron concentration in the Apd1p protein solution was obtained by performing a linear regression on the dataset and deriving an equation  $Y = A + BX$ , where A is the y intercept, B is the slope, Y is the normalized detection signal for iron and X is the iron concentration. The iron concentration in the original Apd1p solution was calculated to be 0.511 mM.

Thus, Apd1p might function as a dimer and contain a [2Fe-2S] cluster.

**HU sensitivity of *apd1Δ* cells is unlikely mediated through dNTP regulatory network.** RNR is a major target of HU<sup>13</sup>. RNR generates DNA building blocks for replication and repair by catalyzing the conversion of NTP to dNTP through a free radical-based mechanism<sup>36,37</sup>. The active form of the RNR small subunit in

budding yeast is a heterodimer of  $\beta$  and  $\beta'$  subunits, encoded by the *RNR2* and *RNR4* genes, respectively<sup>38</sup>.  $\beta$  subunit houses a diferric tyrosyl radical cofactor ( $\text{Fe}_2^{\text{III}}\text{-Tyr}^*$ ) that is essential for initiation of nucleotide reduction in RNR large subunits. This initiation step controls the catalytic activity of the enzyme<sup>37</sup>. In a recent study of the *in vivo* formation of diferric tyrosyl radical in Rnr2p, it was demonstrated that an Fe-S protein, Dre2p, is required for optimal RNR activity and  $\text{Tyr}^*$  generation<sup>23</sup>.

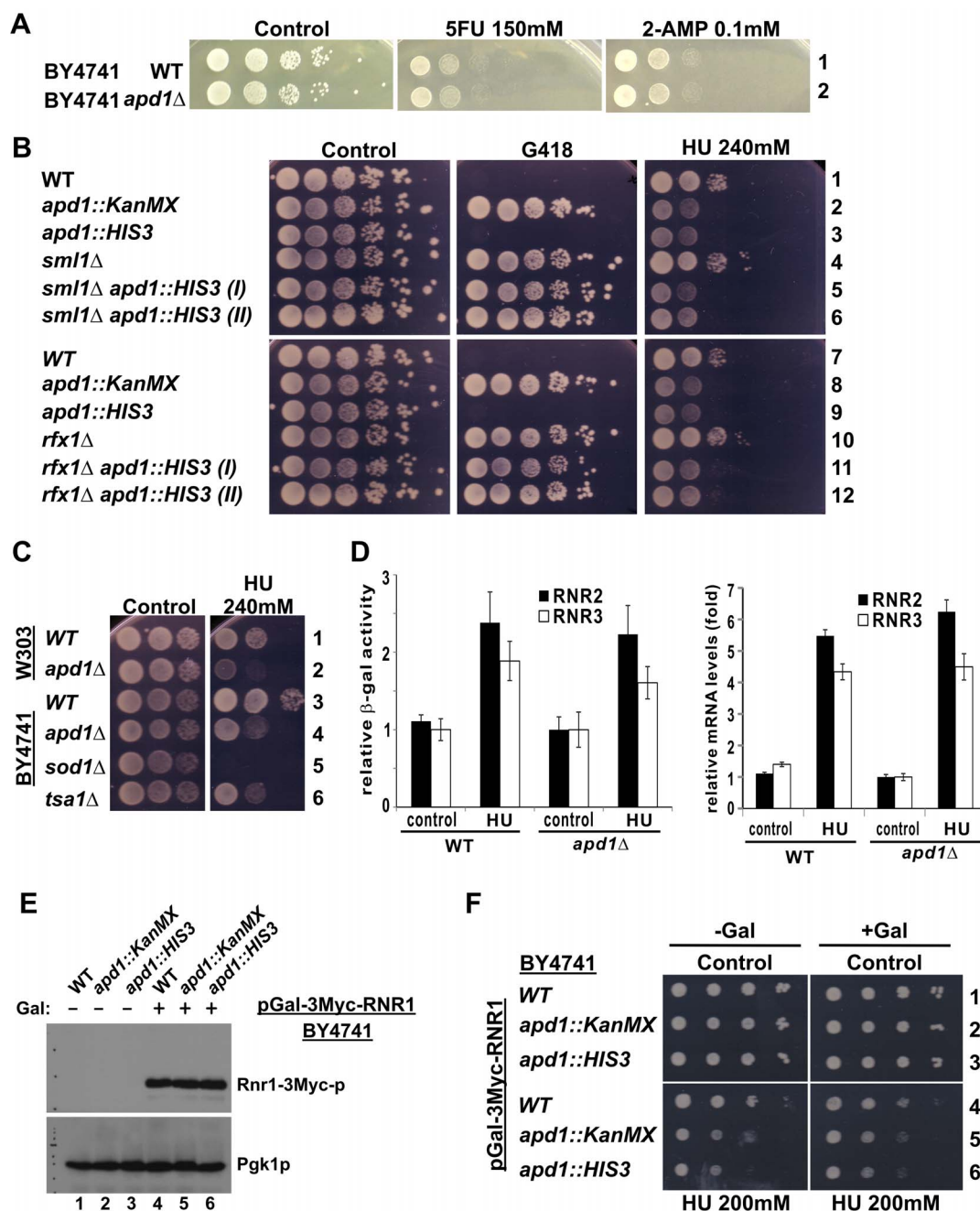


**Figure 5** | HU sensitivity of *apd1Δ* cells is not mediated through dNTP regulatory network. (A) *apd1Δ* cells were not sensitive to nucleotide analogs. Ten-fold serial dilutions of strains BY4741 WT and BY4741 *apd1Δ* were spotted on YPD agar medium containing the indicated dose of 5FU or 2-AMP. Plates were incubated for 3–4 days at 30°C. (B) Deletion of *RNR* negative regulators in *apd1Δ* cells did not affect HU sensitivity. Ten-fold serial dilutions of strains BY4741 WT, BY4741 *apd1Δ*, BY4741 *sml1Δ*, BY4741 *rfx1Δ*, BY4741 *apd1Δsml1Δ* (clones I and II) and BY4741 *apd1Δrfx1Δ* (clones I and II) were spotted on YPD agar medium containing the indicated dose of HU. (C) Loss of *APD1* sensitized cells to HU in both BY4741 and W303 genetic background. Ten-fold serial dilutions of strains W303 WT, W303 *apd1Δ*, BY4741 WT, BY4741 *apd1Δ*, BY4741 *sod1Δ* and BY4741 *tsa1Δ* were spotted on YPD agar medium, containing the indicated dose of HU. (D) Loss of *APD1* did not affect the induction of *RNRs* in the presence of HU. W303 WT and W303 *apd1Δ* cells transformed with pRNR2/3-LacZ reporter were grown in SC-Ura liquid medium containing 50 mM of HU. Cells were collected when OD<sub>600</sub> reached 0.5 and β-galactosidase (β-gal) assay was performed to evaluate *RNR* promoter activity. The pRNR2-LacZ activity recovered from control *apd1Δ* cells was arbitrarily set as 1. For quantitative RT-PCR analysis of *RNR* transcripts, logarithmically growing cells of the indicated strains in YPD were subjected to treatment with HU. Total RNA was extracted and 3 μg of RNA was used for cDNA synthesis. Quantitative PCR was performed to assess the levels of *RNR* transcripts. Relative RNA levels were normalized to the amount of *ACT1* transcript. (E) Galactose-induced expression of Rnr1-3Myc-p. Western blotting was performed with mouse anti-Myc (Roche) and mouse anti-Pgk1p (Invitrogen) antibodies. (F) Overexpression of *RNR1* in *apd1Δ* cells did not influence HU sensitivity. Ten-fold serial dilutions of the indicated strains carrying pGal-3Myc-RNR1 were spotted on SC-Ura medium containing either raffinose (–Gal) or galactose (+Gal) plus 200 mM of HU.



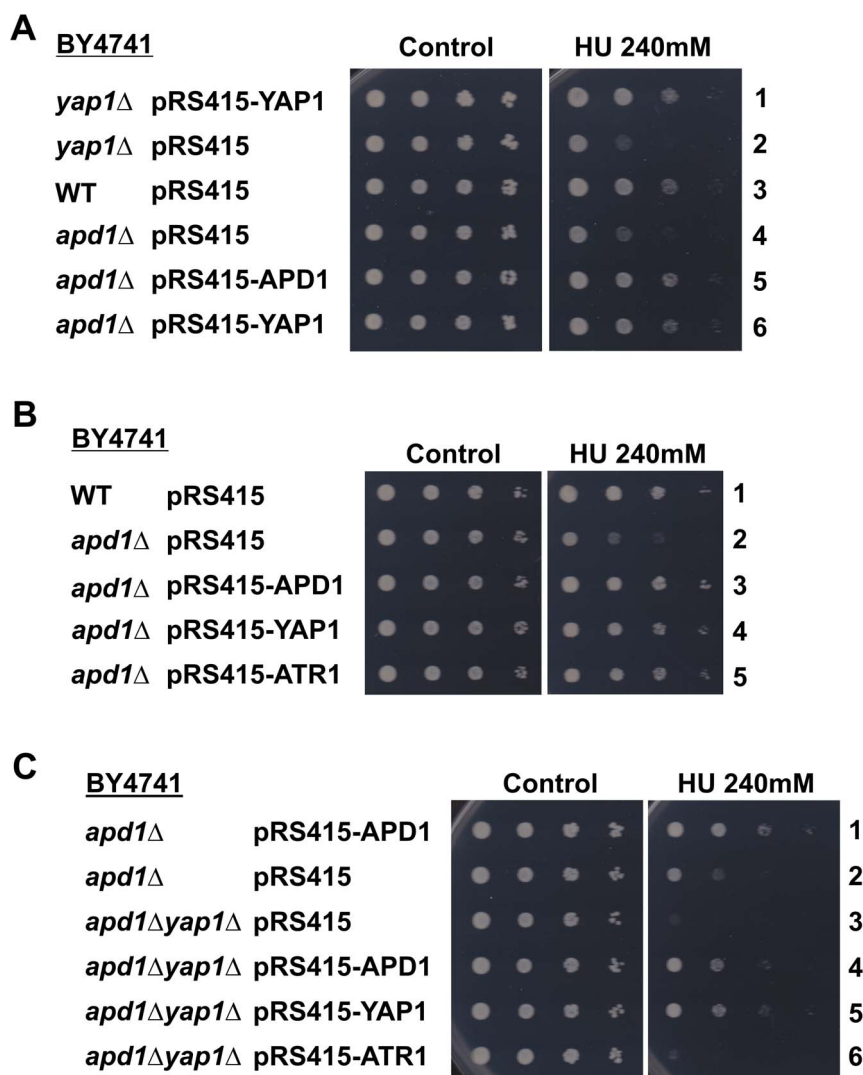


**Figure 6** | Suppression of HU sensitivity in *apd1*Δ cells by *YAP1* and *ATR1*. (A) Expression of *YAP1* rescued the HU sensitivity in *apd1*Δ cells. Ten-fold serial dilutions of strains *yap1*Δ pRS415-*YAP1*, *yap1*Δ pRS415, WT pRS415, *apd1*Δ pRS415, *apd1*Δ pRS415-*APD1* and *apd1*Δ pRS415-*YAP1* were spotted on SC-L medium containing 240 mM of HU. Plates were incubated for 3–4 days at 30°C. (B) Expression of *ATR1* suppressed the HU sensitivity in *apd1*Δ cells. Ten-fold serial dilutions of strains WT pRS415, *apd1*Δ pRS415, *apd1*Δ pRS415-*APD1*, *apd1*Δ pRS415-*YAP1* and *apd1*Δ pRS415-*ATR1* were spotted on SC-L medium containing 240 mM of HU. (C) Suppression of the HU sensitivity in *apd1*Δ cells by *ATR1* was lost in the absence of *YAP1*. Ten-fold serial dilutions of strains *apd1*Δ pRS415-*APD1*, *apd1*Δ pRS415, *apd1*Δ*yap1*Δ pRS415, *apd1*Δ*yap1*Δ pRS415-*APD1*, *apd1*Δ*yap1*Δ pRS415-*YAP1* and *apd1*Δ*yap1*Δ pRS415-*ATR1* were spotted on SC-L medium containing 240 mM of HU.

Since Apd1p is an Fe-S protein and loss of *APD1* resulted in HU sensitivity, we asked whether Apd1p might also play a role in the electron-transfer of RNR in the context of dNTP production. To test this idea, we first determined whether *apd1*Δ cells might be sensitive to other nucleotide analogs 5-flourouracil (5-FU) and adenosine-2'-monophosphate (2-AMP), which serve as inhibitors of dNTP synthesis<sup>39</sup>. Different from the response to HU, *apd1*Δ cells were not sensitive to 5-FU and 2-AMP (Fig. 5A, row 2 compared to 1). To verify this result, we simultaneously deleted *APD1* and either *SML1* or *RFX1*. Sml1p is an RNR inhibitor<sup>40</sup> and Rfx1p is an RNR transcriptional corepressor<sup>41</sup>. If the HU sensitivity in *apd1*Δ cells, as in the case of *tsa1*Δ cells<sup>8</sup>, is mediated through the dNTP regulatory network, it should be rescued when dNTP production is de-repressed in the absence of *SML1* or *RFX1*. However, disruption of *SML1* or *RFX1* did not influence the HU sensitivity in *apd1*Δ cells (Fig. 5B, rows 5, 6, 11 and 12 compared to 2, 3, 8 and 9). Hence, the HU sensitivity in *apd1*Δ cells was unlikely due to dNTP dysregulation.

Besides, we also investigated whether *RNR* genes are induced in the absence of *APD1*. To this end, we examined the transcriptional

induction of *RNR2/3* in *apd1*Δ cells in the backgrounds of both W-303 and BY4741 strains. We first verified that loss of *APD1* sensitized cells to HU (Fig. 5C, row 2 compared to 1 and row 4 compared to 3). In parallel, we also included positive control cells, like *sod1*Δ and *tsa1*Δ, which have been previously been shown<sup>8,42</sup> to be sensitive to HU (Fig. 5C, rows 5–6 compared to 3). Next, transcriptional induction of *RNR2* and *RNR3* were analyzed by *RNR2/3*-*LacZ* reporter constructs<sup>43</sup>. Cells carrying respective reporter constructs were grown in liquid culture and treated with HU. Cells were not sensitive to HU at this low concentration. β-galactosidase assay was performed to measure transcriptional activity of *RNR2* and *RNR3* promoters. In line with results in Fig. 5B, loss of *APD1* did not alter transcriptional induction of *RNR* genes (Fig. 5D, left panel). Consistent with this, induction of *RNR2* transcripts was comparable between WT and *apd1*Δ cells in BY4741 background (Fig. 5D, right panel), indicating that loss of *APD1* did not affect *RNR* transcription. Furthermore, we directly increased the production of dNTP by over-expressing a galactose-inducible *RNR1* gene in *apd1*Δ cells. This construct has previously been shown to dramatically upregulate





dNTP production and thereby contribute to exacerbated mutator phenotype<sup>44,45</sup>. It has also been used to study the relevance of dNTP production to reactive oxygen species-mediated mutagenesis<sup>8</sup>. The expression of Rnr1-3Myc-p was successfully induced with the addition of galactose (Fig. 5E, lanes 4–6 compared to 1–3). Under enforced Rnr1p expression, the HU sensitivity of *apd1Δ* cells remained unchanged (Fig. 5F, rows 5–6 compared to 4), suggesting that the overproduction of dNTP could not rescue the HU phenotype in *apd1Δ* cells. Notably, such sensitivity was unaffected by the *KanMX* gene deletion cassette, as the replacement of *APD1* by *HIS3* also resulted in identical phenotypes (Fig. 5B, rows 2–3 compared to 1 and rows 8–9 compared to 7; Fig. 5F, rows 5–6 compared to 4). Taken together, these results demonstrated that the suppression of HU sensitivity by *APD1* was unlikely mediated through the dNTP regulatory network.

### Suppression of HU sensitivity in *apd1Δ* cells by *YAP1* and *ATR1*.

Since modulation of dNTP production did not affect HU sensitivity in *apd1Δ* cells and our candidate gene approach to identify genetic partners of *APD1* was not fruitful, we performed a genetic screen to search for high-copy-number suppressors of the HU phenotype. An expression library of all yeast genes was used in this screen and *YAP1* was the only gene found to rescue the HU sensitivity in *apd1Δ* cells. A *YAP1* plasmid was isolated from all 11 HU-sensitive clones obtained in the screen. To verify this, we constructed *YAP1* expression plasmid and transformed it into *apd1Δ* cells. As shown in Fig. 6A, ectopic expression of *YAP1* effectively complemented the HU sensitivity in *apd1Δ* cells (Fig. 6A, row 6 compared to 4). This was comparable to the re-expression of *APD1* (Fig. 6A, row 6 compared to 5), indicating that *YAP1* serves as a physiological suppressor of HU sensitivity in *apd1Δ* cells. Notably, *yap1Δ* cells were also sensitive to HU (Fig. 6A, row 2 compared to 3). Re-expression of *YAP1* plasmid successfully rescued such phenotype (Fig. 6A, row 1 compared to 3), indicating the functionality of p*YAP1* expression plasmid in these cells.

One of the known *YAP1* downstream targets is *ATR1*, a multi-drug resistance gene encoding a membrane transporter. Its expression has been shown to be transcriptionally upregulated by *YAP1*<sup>33</sup>. *ATR1* is required for cellular resistance to cytotoxic agents such as aminotriazole and boron.<sup>26,46</sup> To explore whether *ATR1* might also be involved in the suppression of HU sensitivity in *apd1Δ* cells, expression plasmid of *ATR1* was constructed under the regulation of its own promoter. Complementation experiment was carried out. Expression of either *ATR1* or *YAP1* protected the *apd1Δ* cells from HU challenge to full extent as that of *APD1* (Fig. 6B, rows 4–5

compared to 2–3). Thus, both *ATR1* and *YAP1* are fully capable of suppressing the deleterious effect of HU in *APD1*-null cells.

We next investigated the genetic interaction between *ATR1* and *YAP1* in the suppression of HU sensitivity in *apd1Δ* cells. To this end, we generated *apd1Δ yap1Δ* cells. Double deletion of *APD1* and *YAP1* exacerbated the HU sensitivity when compared to individual single mutants (Fig. 6C, row 3 compared to row 2 and to Fig. 6A, row 2), while re-expression of p*APD1* or p*YAP1* reverted the cell growth phenotype back to its counterpart single mutant (Fig. 6C, row 3 compared to 4–5). This indicated the effectiveness and specificity of the genetic targeting. In this genetic background, re-expression of *ATR1* plasmid, under the control of its own promoter, was ineffective in rescuing the HU phenotype (Fig. 6C, row 6 compared to 4–5). Thus, the protective effect of *ATR1* was not seen in the absence of *YAP1*.

### Discussion

We provided two key messages in this study. First, yeast Apd1p is an Fe-S protein. Second, loss of *APD1* confers HU sensitivity. Our findings are consistent with the notion that dimeric Apd1p forms a [2Fe–2S] cluster which mediates its cellular function. As such, disruption of iron-binding motifs in Apd1p abolished its ability to protect cells against HU. Furthermore, the HU sensitivity in *apd1Δ* cells was not mediated through the dNTP regulatory network, but was suppressed by *YAP1* or its target *ATR1*. Our findings revealed a new function of Apd1p in cellular defense against HU, which might be relevant to other thioredoxin-like ferredoxins.

Thioredoxin-like ferredoxins are a large family of Fe-S proteins with unknown biological function<sup>18</sup>. This study was started based on the hypothesis that Apd1p might be the electron donor for Tsa1p, a master peroxiredoxin in yeast<sup>9,10,16</sup>. Although we did not find any physical or genetic interaction between Apd1p and Tsa1p, we characterized Apd1p as an Fe-S protein critically involved in cellular defense against HU. On the other hand, we were unable to verify several results obtained for Apd1p in global analyses of drug susceptibility. Particularly, *apd1Δ* cells were not sensitive to H<sub>2</sub>O<sub>2</sub>. Based on our initial findings, we revised our model to hypothesize that Apd1p might operate through the dNTP regulatory network to exert its protective effect against HU. Although we could not positively define a role for dNTP production in the HU sensitivity of *apd1Δ* cells, we performed a genome-wide screen and identified *YAP1* as a high-copy-number suppressor of the HU phenotype. The new information about Apd1p obtained in our study has provided the foundation for future investigations.

Table 1 | Yeast strains

| Name              | Parent  | Genotype  | Reference |
|-------------------|---------|---|-----------|
| BY4741            |         | <i>MATa his3Δ1 leu2Δ0 met15Δ0 ura3Δ0</i>  | (54)      |
| HMY010            | BY4741  | <i>apd1Δ::HIS3*</i>   | This work |
| HMY011            | BY4741  | <i>apd1Δ::KanMX</i>   | This work |
| HMY012            | BY4741  | <i>Yap1Δ::KanMX4</i>  | This work |
| 512 <sup>a</sup>  | BY4741  | <i>sml1Δ::KanMX4</i>  | (54)      |
| 4125 <sup>a</sup> | BY4741  | <i>rfx1Δ::KanMX4</i>  | (54)      |
| 6913 <sup>a</sup> | BY4741  | <i>sod1Δ::KanMX4</i>  | (54)      |
| HMY001            | BY4741  | <i>tsa1Δ::HIS3*</i>   | (8)       |
| HMY013            | 512     | <i>sml1Δ::KanMX4 apd1Δ::HIS3*</i>   | This work |
| HMY014            | 4125    | <i>rfx1Δ::KanMX4 apd1Δ::HIS3*</i>   | This work |
| HMY015            | HMY012  | <i>yap1Δ::KanMX4 apd1Δ::HIS3*</i>   | This work |
| BY4742            |         | <i>MATx his3Δ1 leu2Δ0 met15Δ0 ura3Δ0</i>  | (54)      |
| HMY016            | BY4742  | <i>apd1Δ::HIS3*</i>   | This work |
| BY4743            |         | <i>MATa/a his3Δ1/his3Δ1 leu2Δ0/leu2Δ0 LYS2/lys2Δ0 met15Δ0/MET15 ura3Δ0/ura3Δ0</i> | (54)      |
| HMY017            | BY4743  | <i>apd1Δ::HIS3*/apd1Δ::HIS3*</i>  | This work |
| W303-1a           |         | <i>MATa ade2 ura3 trp1 leu2 his3 can1</i>   |           |
| HMY018            | W303-1a | <i>apd1Δ::HIS3*</i>   | This work |

<sup>a</sup>Purchased from Research Genetics<sup>54</sup>.  
HIS3\* designates the HIS3 allele from *Saccharomyces kluyveri*.



Table 2 | Oligonucleotide sequences for RT-PCR and site-directed mutagenesis

| Name        | Sequence  | Expected size (bp) |
|-------------|---|--------------------|
| RNR2-RT-F   | ATGCCTAAAGAGACCCCTCCA   | 390                |
| RNR2-RT-R   | CTCGTTTCGTTCACTCTGTGTTC   |                    |
| ACT1-RT-F   | CACCCGTTC TTTGACTGAAGC  | 520                |
| ACT1-RT-R   | TACCGGCAGATCCAAACCC   |                    |
| APD1-RT-F   | ACGAGGGATAAACGATGCGG  | 313                |
| APD1-RT-R   | TTACCAGCTTTGATATTTCTAATAC   |                    |
| ANB1-RT-F   | GTCGACATGTCCACTTCCAAGACCGG  | 244                |
| ANB1-RT-R   | CTGTCACCCAATTCACCTTCTGGTGC  |                    |
| APD1-CX3C-F | GCTGCTAACGAACATAGC(G*GC)TCTGGTGAT(A*GC)AAAACAGAAATTGAAGAAGG         |                    |
| APD1-CX3C-R | CCTTCTCAA TTCTGTTTT(GCT*)ATCACCAGA(GCC*)GCTA T GTTCGTTAGC AGC       |                    |
| APD1-HX3H-F | GGGTGTCAAATTCATTGTTAAT(G*G*T)GTTGGTGGT(A*G*C)AAATTTGCTGCAAATG       |                    |
| APD1-HX3H-R | CATTGCAGC AAATTT(GC*T*)ACCACCAAC(AC*C*)ATTA ACAAAATGCAATTTTG ACACCC |                    |

Nucleotides changed are asterisked and codons involved are parenthesized.

Our analysis of purified Apd1p protein by SDS-PAGE, color visualization, UV-visible spectrophotometric scanning and ICP-MS provided the first experimental evidence in support of the formation of a [2Fe–2S] cluster in Apd1p dimer. Although additional biophysical methods including electron paramagnetic resonance, nuclear magnetic resonance and Mössbauer spectroscopy could be used to characterize Apd1p further<sup>19,47</sup>, our biological assays have already indicated the role of redox and the essentiality of both iron-binding motifs in cellular function of Apd1p. Further investigations are required to shed more mechanistic light on exactly how the [2Fe–2S] cluster in Apd1p could mediate the protection from HU challenge.

Thioredoxins, glutaredoxins and peroxiredoxins serve as redox-sensitive molecular switches in cell signaling<sup>9,16</sup>, which are commonly mediated through the modulation of disulfide bond formation<sup>21,48</sup>. In this regard, our findings on Apd1p are generally consistent with the notion that it might function to modulate disulfide bond formation in its target. Our genetic analysis indicated the ability of Yap1p transcription factor to suppress the HU sensitivity in *apd1Δ* cells. Thus, Yap1p, but neither Tsa1p nor RNR as we originally hypothesized, might be a direct target of Apd1p. It will be of great interest to see how Apd1p might affect the transcriptional activity of Yap1p. Redox regulation of Yap1p by glutathione peroxidase Gpx3p, Tsa1p and Ybp1p has been documented<sup>49–52</sup>. Whether Apd1p might modulate Yap1p and related transcription factors in a similar manner warrants further study.

Our work reveals that the sensitivity of *apd1Δ* cells to HU can be suppressed by *YAPI* or *ATR1*. Although Yap1p is known to play an important role in stress response<sup>31,32</sup> and its expression is activated by HU<sup>34</sup>, we provided the first demonstration of the protective role of Yap1p and Atr1p against HU. Exactly how Yap1p modulates cellular response to HU remains murky. In one perspective, Atr1p is the target of Yap1p in this response since it is also capable of suppressing HU sensitivity in *apd1Δ* cells. However, the inability of *ATR1* to suppress HU sensitivity in *apd1Δ yap1Δ* cells suggests a more complicated picture. The involvement of other Yap1p targets that cooperate with Atr1p is possible. One candidate is the Yap1p-regulated membrane transporter Flr1p, which is already known to mediate resistance to several cytotoxic drugs<sup>27,28,53</sup>. Indeed in some of these cases Flr1p and Atr1p are known to cooperate with each other.<sup>27,28</sup> Alternatively, Yap1p might be absolutely required for expression or activity of Atr1p. In other words, Atr1p might not be expressed in the absence of *YAPI*. In our genetic analysis, *YAPI* was found to rescue HU sensitivity in *apd1Δ* cells. In addition, *apd1Δ yap1Δ* cells were more sensitive to HU than *apd1Δ* or *yap1Δ* cells. These results raised the possibility that *YAPI* and *APD1* might operate in different pathways that confer resistance to HU. Nevertheless, additional biochemical and genetic analyses are required to clarify the roles of Yap1p and Atr1p in cellular defense against HU.

## Methods

**Strains and plasmids.** *Saccharomyces cerevisiae* strains BY4741<sup>54</sup> and W303-1a, and their isogenic strains (Table 1) were used. All knockout mutants were constructed by one-step gene deletion method<sup>55</sup>. Primers were listed in Table 2. Expression vector for *APD1*, *YAPI* and *ATR1* was based on pRS415 and the gene locus including promoter and open reading frame was PCR-amplified from yeast genomic DNA. Expression plasmids for *APD1* mutants were constructed by site-directed mutagenesis as described<sup>18,56,57</sup>. The Myc tag sequence in *APD1* and its mutants was introduced by PCR.

Plasmids pGal-RNR1, pRNR2-LacZ and pRNR3-LacZ were kindly provided by Dr. Stephen Elledge<sup>38,43</sup>.

**RNA analysis.** Total RNA was extracted by phenol/freeze RNA preparation method as described<sup>58</sup>. For RT-PCR, 3 μg of total RNA was used for cDNA synthesis. Quantitative RT-PCR was performed as described<sup>59</sup>. Relative mRNA levels were normalized to *ACT1*. PCR primers were listed in Table 2.

**Protein analysis.** Western blotting was performed essentially as described<sup>18,42,57</sup>. Yeast cells were harvested by centrifugation, followed by trichloroacetic acid extraction with the help of glass beads. β-galactosidase assay was carried out using a chemiluminescent method as described<sup>57</sup>.

**Cell growth and cell cycle profiling.** For growth curve analysis, logarithmically growing yeast cells, BY4741 wild type (WT) and *apd1Δ*, were inoculated into YPD medium to an OD<sub>600</sub> of 0.1. Every indicated time point thereafter, cell density was monitored by OD<sub>600</sub>. Cell cycle profiling was performed as described previously<sup>60</sup>. First, yeast cells were grown to a density of 5 × 10<sup>7</sup> cells/ml in YPD medium. Cells were spun down and washed in PBS. Cells were then fixed in 1 ml of 70% ethanol for 1 hour at 4 °C in dark. Subsequently, the fixed cells were treated with RNase A at 37 °C for 1 hour. Cells were pelleted and resuspended in 1 ml of PBS containing 50 μg/ml propidium iodide. Samples were kept in dark at room temperature for 1 hour prior to flow cytometric analysis. DNA content of 20,000 cells from each sample was analyzed. To measure intracellular reactive oxygen species, cells were treated with 0.5 mM H<sub>2</sub>O<sub>2</sub> and then with 10 μM DCF as described<sup>60</sup>.

**Expression and purification of recombinant Apd1p.** Bacterially expressed recombinant His-Apd1p was purified with the Ni-NTA-Superflow resin. Proteins were eluted and subjected to 15% SDS-PAGE (for Apd1p WT) or 15% non-denaturing PAGE (for Apd1p WT, CX<sub>3</sub>C and HX<sub>3</sub>H). After electrophoresis, the SDS-PAGE gel was stained with Coomassie blue to visualize the purified protein. The colored Apd1p band was directly seen on the non-denaturing gel.

**UV-visible spectroscopy of recombinant Apd1p proteins.** Each of the purified proteins was subjected to photometric scanning with a wavelength range of 260 to 750 nm and a scanning step size of 2 nm in 100 ms on a Varioskan™ Flash spectrometer.

**Determination of iron concentration by ICP-MS.** The concentration of Apd1p used for ICP-MS analysis was determined by bicinchoninic acid (BCA) micro-scale assay (Novagen) using bovine serum albumin (BSA) as a standard. Apd1p protein sample was diluted 50-fold prior to analysis. Calibration curve was obtained by measuring a set of iron standards (Fluka) ranging from 30 to 90 ppb (R = 0.9995). ICP-MS experiments were performed on an Agilent 7500a spectrometer (Agilent Technologies).

- Entian, K. D. *et al.* Functional analysis of 150 deletion mutants in *Saccharomyces cerevisiae* by a systematic approach. *Mol Gen Genet* **262**, 683–702 (1999).
- Blackman, R. K. *et al.* Mitochondrial electron transport is the cellular target of the oncology drug elesclomol. *PLoS One* **7**, e29798 (2012).



3. Postma, L., Lehrach, H. & Ralser, M. Surviving in the cold: yeast mutants with extended hibernating lifespan are oxidant sensitive. *Aging* **1**, 957–960 (2009).
4. Huh, W. K. *et al.* Global analysis of protein localization in budding yeast. *Nature* **425**, 686–691 (2003).
5. Krogan, N. J. *et al.* Global landscape of protein complexes in the yeast *Saccharomyces cerevisiae*. *Nature* **440**, 637–643 (2006).
6. Huang, M. E., Rio, A. G., Nicolas, A. & Kolodner, R. D. A genomewide screen in *Saccharomyces cerevisiae* for genes that suppress the accumulation of mutations. *Proc Natl Acad Sci USA* **100**, 11529–11534 (2003).
7. Huang, M. E. & Kolodner, R. D. A biological network in *Saccharomyces cerevisiae* prevents the deleterious effects of endogenous oxidative DNA damage. *Mol Cell* **17**, 709–720 (2005).
8. Tang, H. M. V., Siu, K. L., Wong, C. M. & Jin, D. Y. Loss of yeast peroxiredoxin Tsa1p induces genome instability through activation of the DNA damage checkpoint and elevation of dNTP levels. *PLoS Genet* **5**, e1000697 (2009).
9. Rhee, S. G., Chae, H. Z. & Kim, K. Peroxiredoxins: a historical overview and speculative preview of novel mechanisms and emerging concepts in cell signaling. *Free Radic Biol Med* **38**, 1543–1552 (2005).
10. Rhee, S. G., Woo, H. A., Kil, I. S. & Bae, S. H. Peroxiredoxin functions as a peroxidase and a regulator and sensor of local peroxides. *J Biol Chem* **287**, 4403–4410 (2012).
11. Nyström, T., Yang, J. & Molin, M. Peroxiredoxins, gerontogenes linking aging to genome instability and cancer. *Genes Dev* **26**, 2001–2008 (2012).
12. Yarbro, J. W. Mechanism of action of hydroxyurea. *Semin Oncol* **19**, 1–10 (1992).
13. Hofer, A., Crona, M., Logan, D. T. & Sjöberg, B. M. DNA building blocks: keeping control of manufacture. *Crit Rev Biochem Mol Biol* **47**, 50–63 (2012).
14. Madaan, K., Kaushik, D. & Verma, T. Hydroxyurea: a key player in cancer chemotherapy. *Expert Rev Anticancer Ther* **12**, 19–29 (2012).
15. Meyer, Y., Buchanan, B. B., Vignols, F. & Reichheld, J. P. Thioredoxins and glutaredoxins: unifying elements in redox biology. *Annu Rev Genet* **43**, 335–367 (2009).
16. Hanschmann, E. M., Godoy, J. R., Berndt, C., Hudemann, C. & Lillig, C. H. Thioredoxins, glutaredoxins, and peroxiredoxins - molecular mechanisms and health significance: from cofactors to antioxidants to redox signaling. *Antioxid Redox Signal* **19**, 1539–1605 (2013).
17. Chae, H. Z., Chung, S. J. & Rhee, S. G. Thioredoxin-dependent peroxide reductase from yeast. *J Biol Chem* **269**, 27670–27678 (1994).
18. Meyer, J. Ferredoxins of the third kind. *FEBS Lett* **509**, 1–5 (2001).
19. Xu, X. M. & Möller, S. G. Iron-sulfur clusters: biogenesis, molecular mechanisms, and their functional significance. *Antioxid Redox Signal* **15**, 271–307 (2011).
20. Pedone, E., Limauro, D., D'Ambrosio, K., De Simone, G. & Bartolucci, S. Multiple catalytically active thioredoxin folds: a winning strategy for many functions. *Cell Mol Life Sci* **67**, 3797–3814 (2010).
21. Groitl, B. & Jakob, U. Thiol-based redox switches. *Biochim Biophys Acta* **1844**, 1335–1343 (2014).
22. Wu, C. H., Jiang, W., Krebs, C. & Stubbe, J. YfaE, a ferredoxin involved in diferrityrosyl radical maintenance in *Escherichia coli* ribonucleotide reductase. *Biochemistry* **46**, 11577–11588 (2007).
23. Zhang, Y. *et al.* Investigation of in vivo diferrityrosyl radical formation in *Saccharomyces cerevisiae* Rnr2 protein: requirement of Rnr4 and contribution of Grx3/4 AND Dre2 proteins. *J Biol Chem* **286**, 41499–41509 (2011).
24. Wysocki, R. *et al.* Transcriptional activation of metalloids tolerance genes in *Saccharomyces cerevisiae* requires the AP-1-like proteins Yap1p and Yap8p. *Mol Biol Cell* **15**, 2049–2060 (2004).
25. Viau, C. *et al.* Sensitivity to Sn<sup>2+</sup> of the yeast *Saccharomyces cerevisiae* depends on general energy metabolism, metal transport, anti-oxidative defences, and DNA repair. *Biomaterials* **19**, 705–714 (2006).
26. Kaya, A., Karakaya, H. C., Fomenko, D. E., Gladyshev, V. N. & Koc, A. Identification of a novel system for boron transport: Atr1 is a main boron exporter in yeast. *Mol Cell Biol* **29**, 3665–3674 (2009).
27. Sundström, L., Larsson, S. & Jönsson, L. J. Identification of *Saccharomyces cerevisiae* genes involved in the resistance to phenolic fermentation inhibitors. *Appl Biochem Biotechnol* **161**, 106–115 (2010).
28. Westman, J. O., Manikonda, R. B., Franzén, C. J. & Taherzadeh, M. J. Encapsulation-induced stress helps *Saccharomyces cerevisiae* resist convertible lignocellulose derived inhibitors. *Int J Mol Sci* **13**, 11881–11894 (2012).
29. Kim, D. & Hahn, J. S. Roles of the Yap1 transcription factor and antioxidants in *Saccharomyces cerevisiae*'s tolerance to furfural and 5-hydroxymethylfurfural, which function as thiol-reactive electrophiles generating oxidative stress. *Appl Environ Microbiol* **79**, 5069–5077 (2013).
30. Pimentel, C. *et al.* Yap1 mediates tolerance to cobalt toxicity in the yeast *Saccharomyces cerevisiae*. *Biochim Biophys Acta* **1840**, 1977–1986 (2014).
31. Lee, J. *et al.* Yap1 and Skn7 control two specialized oxidative stress response regulons in yeast. *J Biol Chem* **274**, 16040–16046 (1999).
32. Toone, W. M., Morgan, B. A. & Jones, N. Redox control of AP-1-like factors in yeast and beyond. *Oncogene* **20**, 2336–2346 (2001).
33. Coleman, S. T., Tseng, E. & Moye-Rowley, W. S. *Saccharomyces cerevisiae* basic region-leucine zipper protein regulatory networks converge at the ATR1 structural gene. *J Biol Chem* **272**, 23224–23230 (1997).
34. Dubacq, C. *et al.* Role of the iron mobilization and oxidative stress regulons in the genomic response of yeast to hydroxyurea. *Mol Genet Genomics* **275**, 114–124 (2006).
35. Smith, S. *et al.* Mutator genes for suppression of gross chromosomal rearrangements identified by a genome-wide screening in *Saccharomyces cerevisiae*. *Proc Natl Acad Sci USA* **101**, 9039–9044 (2004).
36. Stubbe, J. & van Der Donk, W. A. Protein radicals in enzyme catalysis. *Chem Rev* **98**, 705–762 (1998).
37. Nordlund, P. & Reichard, P. Ribonucleotide reductases. *Annu Rev Biochem* **75**, 681–706 (2006).
38. Huang, M. & Elledge, S. J. Identification of RNR4, encoding a second essential small subunit of ribonucleotide reductase in *Saccharomyces cerevisiae*. *Mol Cell Biol* **17**, 6105–6113 (1997).
39. Longley, D. B., Harkin, D. P. & Johnston, P. G. 5-fluorouracil: mechanisms of action and clinical strategies. *Nat Rev Cancer* **3**, 330–338 (2003).
40. Chabes, A., Domkin, V. & Thelander, L. Yeast Sml1, a protein inhibitor of ribonucleotide reductase. *J Biol Chem* **274**, 36679–36683 (1999).
41. Huang, M., Zhou, Z. & Elledge, S. J. The DNA replication and damage checkpoint pathways induce transcription by inhibition of the Crt1 repressor. *Cell* **94**, 595–605 (1998).
42. Carter, C. D., Kitchen, L. E., Au, W. C., Babic, C. M. & Basrai, M. A. Loss of SOD1 and LYS7 sensitizes *Saccharomyces cerevisiae* to hydroxyurea and DNA damage agents and downregulates MEC1 pathway effectors. *Mol Cell Biol* **25**, 10273–10285 (2005).
43. Zhou, Z. & Elledge, S. J. Isolation of crt mutants constitutive for transcription of the DNA damage inducible gene RNR3 in *Saccharomyces cerevisiae*. *Genetics* **131**, 851–866 (1992).
44. Chabes, A. *et al.* Survival of DNA damage in yeast directly depends on increased dNTP levels allowed by relaxed feedback inhibition of ribonucleotide reductase. *Cell* **112**, 391–401 (2003).
45. Chabes, A. & Stillman, B. Constitutively high dNTP concentration inhibits cell cycle progression and the DNA damage checkpoint in yeast *Saccharomyces cerevisiae*. *Proc Natl Acad Sci USA* **104**, 1183–1188 (2007).
46. Kanazawa, S., Driscoll, M. & Struhl, K. ATR1, a *Saccharomyces cerevisiae* gene encoding a transmembrane protein required for aminotriazole resistance. *Mol Cell Biol* **8**, 664–673 (1988).
47. Zhang, B. *et al.* Monothiol glutaredoxins can bind linear [Fe<sub>3</sub>S<sub>4</sub>]<sup>+</sup> and [Fe<sub>4</sub>S<sub>4</sub>]<sup>2+</sup> clusters in addition to [Fe<sub>2</sub>S<sub>2</sub>]<sup>2+</sup> clusters: spectroscopic characterization and functional implications. *J Am Chem Soc* **135**, 15153–15164 (2013).
48. König, J., Muthuramalingam, M. & Dietz, K. J. Mechanisms and dynamics in the thiol/disulfide redox regulatory network: transmitters, sensors and targets. *Curr Opin Plant Biol* **15**, 261–268 (2012).
49. Delaunay, A., Pflieger, D., Barrault, M. B., Vinh, J. & Toledano, M. B. A thiol peroxidase is an H<sub>2</sub>O<sub>2</sub> receptor and redox-transducer in gene activation. *Cell* **111**, 471–481 (2002).
50. Veal, E. A., Ross, S. J., Malakasi, P., Peacock, E. & Morgan, B. A. Ybp1 is required for the hydrogen peroxide-induced oxidation of the Yap1 transcription factor. *J Biol Chem* **278**, 30896–30904 (2003).
51. Okazaki, S., Tachibana, T., Naganuma, A., Mano, N. & Kuge, S. Multistep disulfide bond formation in Yap1 is required for sensing and transduction of H<sub>2</sub>O<sub>2</sub> stress signal. *Mol Cell* **27**, 675–688 (2007).
52. Tachibana, T. *et al.* A major peroxiredoxin-induced activation of Yap1 transcription factor is mediated by reduction-sensitive disulfide bonds and reveals a low level of transcriptional activation. *J Biol Chem* **284**, 4464–4472 (2009).
53. Oskouian, B. & Saba, J. D. YAP1 confers resistance to the fatty acid synthase inhibitor cerulenin through the transporter Flr1p in *Saccharomyces cerevisiae*. *Mol Genet Genet* **261**, 346–353 (1999).
54. Winzler, E. A. *et al.* Functional characterization of the *S. cerevisiae* genome by gene deletion and parallel analysis. *Science* **285**, 901–906 (1999).
55. Longtine, M. S. *et al.* Additional modules for versatile and economical PCR-based gene deletion and modification in *Saccharomyces cerevisiae*. *Yeast* **14**, 953–961 (1998).
56. Wong, C. M., Siu, K. L. & Jin, D. Y. Peroxiredoxin-null yeast cells are hypersensitive to oxidative stress and genomically unstable. *J Biol Chem* **279**, 23207–23213 (2004).
57. Kong, K. Y. E. *et al.* Cotranscriptional recruitment of yeast TRAMP complex to intronic sequences promotes optimal pre-mRNA splicing. *Nucl Acids Res* **42**, 643–660 (2014).
58. Schmitt, M. E., Brown, T. A. & Trumppower, B. L. A rapid and simple method for preparation of RNA from *Saccharomyces cerevisiae*. *Nucl Acids Res* **18**, 3091–3092 (1990).
59. Tang, H. M. V. *et al.* Requirement of CRTCI1 coactivator for hepatitis B virus transcription. *Nucl Acids Res* doi:10.1093/nar/gku925 (2014).
60. Wong, C. M., Zhou, Y., Ng, R. W. M., Kung, H. F. & Jin, D. Y. Cooperation of yeast peroxiredoxins Tsa1p and Tsa2p in the cellular defense against oxidative and nitrosative stress. *J Biol Chem* **277**, 5385–5394 (2002).

## Acknowledgments

We thank Drs. Stephen Elledge and Mark Longtine for reagents, and members of Jin laboratory for critical reading of manuscript. This work was supported by grants from the National Natural Science Foundation of China (Young Researcher Award 31200931 to H.-M.V.T.), S.K. Yee Medical Research Fund (2011 to D.-Y.J.), and Fogarty International Center of National Institutes of Health (R01TW008298 to C.-M.W.).



## Author contributions

H.M.V.T., H.Z.S., C.M.W. and D.Y.J. designed the experiments, analyzed data and wrote the manuscript. H.M.V.T., K.P., K.Y.E.K., L.H., L.C.C. and K.L.S. performed the experiments and analyzed data.

## Additional information

**Supplementary information** accompanies this paper at <http://www.nature.com/scientificreports>

**Competing financial interests:** The authors declare no competing financial interests.

**How to cite this article:** Tang, H.-M.V. *et al.* Loss of *APD1* in Yeast Confers Hydroxyurea Sensitivity Suppressed by Yap1p Transcription Factor. *Sci. Rep.* 5, 7897; DOI:10.1038/srep07897 (2015).



This work is licensed under a Creative Commons Attribution-NonCommercial-NoDerivs 4.0 International License. The images or other third party material in this article are included in the article's Creative Commons license, unless indicated otherwise in the credit line; if the material is not included under the Creative Commons license, users will need to obtain permission from the license holder in order to reproduce the material. To view a copy of this license, visit <http://creativecommons.org/licenses/by-nc-nd/4.0/>